SOUTHAMPTON OCEANOGRAPHY CENTRE

INTERNAL DOCUMENT No. 69

Airflow distortion at instrument sites on the FS *Polarstern*

D I Berry, B I Moat & M J Yelland

2001

James Rennell Division for Ocean Circulation and Climate
Southampton Oceanography Centre
University of Southampton
Waterfront Campus
European Way
Southampton
Hants SO14 3ZH
UK

Tel: +44 (0)23 8059 6406
Fax: +44 (0)23 8059 6204
Email: bim@soc.soton.ac.uk

DOCUMENT DATA SHEET

AUTHOR

BERRY, D I, MOAT, B I & YELLAND, M J

PUBLICATION DATE

2001

TITLE

Airflow distortion at instrument sites on the FS *Polarstern*.

REFERENCE

Southampton Oceanography Centre Internal Document, No. 69, 36pp. (Unpublished manuscript)

ABSTRACT

Wind speed measurements obtained from research ships are prone to systematic errors caused by the distortion of the air flow around the ship's hull and superstructure. In this report the air flow around the FS *Polarstern* is simulated for a wind speed of 15 ms^{-1} blowing directly over the bows of the ship using Computational Fluid Dynamics (CFD). The airflow distortion at five anemometer sites has been quantified. All anemometers in this study were located on the lattice mast attached to the crane on the forecastle. The crane was extended in two positions with the anemometers 11.2m and 14.2m forward of the bows. All the anemometers experienced moderate to severe flow distortion, with the wind speed being decelerated by 6 % to 15 % depending on the instrument location. The flow had been displaced vertically by between 0.1m and 0.7m, with the displacement increasing with height.

KEYWORDS

AIRFLOW DISTORTION, COMPUTATIONAL FLUID DYNAMICS, CFD, *POLARSTERN*, WIND SPEED MEASUREMENT

ISSUING ORGANISATION

Southampton Oceanography Centre
University of Southampton
Waterfront Campus
European Way
Southampton SO14 3ZH
UK

AIRFLOW DISTORTION AT INSTRUMENT SITES ON THE *F. S. POLARSTERN*

CONTENTS

1. Introduction 1

2. Description of the *F.S. Polarstern* model 1

3. The air flow at the instrument sites 11.2 m forward of the bow 2

3.a The instrument locations 2

3.b The vertical displacement of the flow 2

3.c The free stream velocity 4

3.d The effect of flow distortion on wind speed 5

4. The air flow at the instrument sites 14.2 m forward of the bow 7

4.a The instrument locations 7

4.b The vertical displacement and velocity error 7

5. Summary 11

6. References 15

7. Figures 16

8. Appendix 31

AIRFLOW DISTORTION AT INSTRUMENT SITES ON THE *F.S. POLARSTERN*

Berry, D. I., B. I. Moat and M. J. Yelland

April 2001

1. Introduction

This report describes an investigation of the air flow distortion around the *F.S. Polarstern*. The Computational Fluid Dynamics (CFD) package VECTIS was used to simulate the flow of air directly over the bow of the ship. Section 2 gives a brief description of the model. The instrument sites examined are those on the lattice mast attached to the crane on the forecastle. The flow distortion at these instrument sites is examined and the wind speed errors produced. The vertical displacement of the flow to each site is also calculated. The lattice mast was deployed in two positions; Section 3 describes the results for the lattice tower when positioned 11.2 m forward of the bow and Section 4 describes the results when the tower was positioned 14.2 m forward of the bow. These results are summarised and discussed in Section 5.

2. Description of the *F.S. Polarstern* model

Figure 1 shows the modelled geometry of the *F.S. Polarstern* with the main instrumentation sites on the lattice mast indicated by crosses. The ship geometry was enclosed in the centre of a 'wind tunnel' or computational volume 800 m long (-400 m < x < 400 m), 600 m wide (-300 m < y < 300 m) and 200 m high (0 m < z < 200 m). The centreline of the ship was parallel to the x-axis at z = 0 m. A logarithmic wind profile was specified at the inlet with a 10 m wind speed of 15 ms^{-1}. The computational volume was split into two domains and a parallel solution generated using two processors. Whilst the computational solver was running the velocities at eight locations were monitored, seven abeam of the ship in the free stream flow and one at an anemometer location. The data from these points show the solution had converged after approximately 19600 times steps with the velocities at the monitoring points constant to the fourth significant figure. The locations of the monitoring points are shown schematically in Figure 2, and Figure 3 shows the velocity data for the last 250 time steps. Once the model had converged a post-processing file was written for the extraction of data throughout the computational volume. Illustrations of the output can be found in the Appendix and a detailed description of the data extraction and analysis can be found in Moat *et al.,* (1996).

The flow in the tunnel was examined to confirm that free stream conditions existed at the sides and ends of the tunnel, i.e. that the presence of the ship did not cause a significant blockage of the flow to these regions. Figure 4a shows the variation in velocity along the tunnel at x = ±350 m, at heights of 10, 20, 30 and 50 m on a plane at y = 250 m, i.e. towards one side of the tunnel. Equivalent data were also extracted from the other side of the tunnel, at y = -250 m, and identical results were found. The central section is shown in more detail in Figure 4b, with the velocity data shown directly abeam of the ship on a plane at y = 250 m and x = ±80 m. The change in velocities at heights of 10 m and 20 m on this plane along the length of the ship are 0.08 ms^{-1} and 0.014 ms^{-1} respectively. These results show that the blockage of the tunnel is minimal. However, since the changes are not zero, the free stream velocity for a particular instrument site is estimated using the vertical profile of velocity about 250 m directly abeam of the instrument site, rather than the profiles at the inlet or outlet of the tunnel.

3. The air flow at the instrument sites 11.2 m forward of the bow

3.a The instrument locations

The locations of the instruments on the lattice tower are shown relative to the lattice tower in Figure 5. It must be noted that the lattice tower itself was not modelled since its open lattice design was too fine to be resolved properly in the model.

In the VECTIS co-ordinates system (where the origin is in the centre of the ship at sea level), the instrument positions ("P" in Tables 1 to 5) are;

SONIC#1	x = 70.57 m	y = 0.25 m	z = 3.80 m
SONIC#2	x = 70.57 m	y = 0.25 m	z = 5.40 m
SONIC#3	x = 70.57 m	y = 0.25 m	z = 8.00 m
SONIC#4	x = 70.57 m	y = 0.25 m	z = 13.00 m
SONIC#5	x = 70.57 m	y = 0.25 m	z = 20.00 m

3.b The vertical displacement of the flow

To calculate the vertical displacement of the flow reaching the instrument a streamline is traced from the inlet of the tunnel to the instrument site (see Figure A5 in the Appendix). Table 1 gives the co-ordinates of; "P" the SONIC#1 instrument site, "P_{stream}" which is the point on the streamline closest to the anemometer, and the origin of the streamline "P_{origin}". It can be seen that the streamline is displaced

vertically by 0.161 m by the time it reaches the approximate position of the anemometer site. Tables 2 to 5 give the equivalent information for the SONIC#2 to SONIC#5 anemometers respectively.

Location	x (m)	y (m)	z (m)
P (SONIC#1)	70.57	0.25	3.8
P_{stream}	70.57	0.25	3.80
$P-P_{stream}$	0.00	0.00	0.00
P_{origin}	398.20	0.25	3.64
$P_{stream}-P_{origin}$			$\Delta z=0.16$

Table 1 The vertical displacement, Δz, of the flow to the SONIC#1 anemometer.

Location	x (m)	y (m)	z (m)
P (SONIC#2)	70.57	0.25	5.40
P_{stream}	70.57	0.25	5.39
$P-P_{stream}$	0.00	0.00	0.01
P_{origin}	396.44	0.25	5.21
$P_{stream}-P_{origin}$			$\Delta z=0.18$

Table 2 The vertical displacement, Δz, of the flow to the SONIC#2 anemometer.

Location	x (m)	y (m)	z (m)
P (SONIC#3)	70.57	0.25	8.00
P_{stream}	70.57	0.25	8.00
$P-P_{stream}$	0.00	0.00	0.00
P_{origin}	396.60	0.25	7.77
$P_{stream}-P_{origin}$			$\Delta z=0.23$

Table 3 The vertical displacement, Δz, of the flow to the SONIC#3 anemometer.

Location	x (m)	y (m)	z (m)
P (SONIC#4)	70.57	0.25	13.00
P_{stream}	70.57	0.25	13.01
$P-P_{stream}$	0.00	0.00	-0.01
P_{origin}	396.49	0.25	12.60
$P_{stream}-P_{origin}$			$\Delta z=0.41$

Table 4 The vertical displacement, Δz, of the flow to the SONIC#4 anemometer.

Location	x (m)	y (m)	z (m)
P (SONIC#5)	70.57	0.25	20.00
P_{stream}	70.57	0.25	20.00
$P-P_{stream}$	0.00	0.00	0.00
P_{origin}	392.97	0.25	19.32
$P_{stream}-P_{origin}$			$\Delta z=0.68$

Table 5 The vertical displacement, Δz, of the flow to the SONIC#5 anemometer.

3.c The free stream velocity

The estimates of the vertical displacement are used to obtain the free stream velocities for the instrument sites. The air parcel reaching the instrument will have originated at a height of ($z-\Delta z$), where z is the anemometer height, and the free stream velocity is obtained at that height on the free steam profile. The velocity of the flow at the instrument site is then compared to the free stream velocity to give the wind speed error.

Figure 6 shows part of the free stream profile near the wind tunnel wall, directly abeam of the SONIC#1 anemometer, at (x = 70.57 m, y = 250 m, 0 m < z < 200 m). This indicates a free steam velocity of 13.81 ms^{-1} at a height of 3.64 m. Free stream velocities were obtained in a similar fashion for the other instrument sites and the results are included in Table 6.

Instrument site	Velocity from each direction	Average velocity (ms^{-1})	Free stream velocity (ms^{-1})	% Error
SONIC#1	11.710(x) 11.710(y) 11.728(z)	11.716	13.809	-15.16 ± 0.20
SONIC#2	12.232(x) 12.231(y) 12.246(z)	12.236	14.204	-13.85 ± 0.26
SONIC#3	12.836(x) 12.835(y) 12.848(z)	12.840	14.711	-12.72 ± 0.30
SONIC#4	13.740(x) 13.729(y) 13.734(z)	13.734	15.344	-10.49 ± 0.15
SONIC#5	14.983(x) 14.982(y) 14.990(z)	14.985	15.946	-6.03 ± 0.11

Table 6 Wind speed errors at the instrument sites 11.2 m forward of the bow.

3.d The effect of flow distortion on wind speed

The free stream flow has small, predictable gradients and can be estimated accurately at any given point on the vertical profile. In contrast, the flow at the instrument site can suffer from severe distortion and large gradients in the velocity field. Additionally it is not always possible to define the mesh so that the instruments are at the exact centres of the computational cells (see Moat *et al.*, 1996). Therefore the velocity at an instrument site is estimated from lines of data extracted in all three directions. Figures 7 to 11 show the lines of data through the instrument sites, and the results are summarised in Table 6. The velocity error at the instrument site (of height z) is expressed as a percentage of the free stream velocity (at height $z-\Delta z$) with a positive error indicating an acceleration of the flow.

The small kinks in the vertical profiles of velocity (e.g. Figure 7c at a height of approximately 1.8 m) are due to the mesh resolution. Figure 12 shows the mesh density around the anemometer sites. It can

be seen that the size of the computational cells increases rapidly with distance upwind of the anemometer sites. Upwind of the instruments the vertical gradient of the velocity is steep, particularly near the surface, and the mesh is too coarse to resolve this profile smoothly. Nearer the instrument sites the mesh is finer, but the "kink" near the surface has not yet become smoothed out. It is clear that this problem will be worse when the anemometers are held further upwind, at a distance of 14.2 m (Section 4). However, fitting smooth curves through each vertical profile showed that the estimates of the wind speeds at the anemometer sites were not seriously affected. The worst cases were found to be nearer the surface with the maximum bias in the wind speed estimated at less than 0.05 ms^{-1}.

Instrument site	Velocity data line	Rate of change of velocity per metre (ms^{-1}/m)	Rate of change of velocity per cell (ms^{-1}/cell)
SONIC#1	Along (x)	0.159	0.014
	Across (y)	0.002	0
	Up (z)	0.353	0.032
SONIC#2	Along (x)	0.149	0.013
	Across (y)	0.001	0
	Up (z)	0.279	0.025
SONIC#3	Along (x)	0.137	0.012
	Across (y)	-0.001	0
	Up (z)	0.241	0.024
SONIC#4	Along (x)	0.075	0.005
	Across (y)	0.013	0.001
	Up (z)	0.030	0.008
SONIC#5	Along (x)	0.021	0.002
	Across (y)	-0.002	0
	Up (z)	0.14	0.013

Table 7 Rate of change of velocity close to the anemometer sites 11.2 m forward of the bow.

An indication of the accuracy of the flow and the severity of the flow distortion is also given by estimates of the gradient of the flow. Estimates of the gradient of the flow are made from Figures 7 to 11 and the rates of change for all the instruments, per metre and per cell, are given in Table 7. The rate of

change per metre in the x-direction is relatively large at the lower positions (SONIC#1 to SONIC#3) suggesting that the flow at these sites is strongly influenced by the presence of the bow. This is confirmed by the severe deceleration of the flow reaching these instrument sites. The flow reaching the SONIC#1 site is decelerated by 15.16%. The deceleration of the flow reaching the SONIC#2 and SONIC#3 sites is slightly less severe but only decreases slowly with height to 12.72 % at the SONIC#3 site. At the SONIC#4 site the flow is disturbed by the presence of the bow to a lesser degree (decelerated by 10.49 %), but the influence of the crane can clearly be seen to cause a severe deceleration of the flow between 14.5 m and 15 m height (Figure 10c). Away from the presence of the bow and the crane the deceleration drops to 6.03% at the SONIC#5 site.

4. The air flow at the instrument sites 14.2 m forward of the bow

4.a The instrument locations

This section summarises the results for the anemometer sites 14.2 m forward of the bow. The extension of the crane from 11.2 m to 14.2 m has not been modelled. The results are summarised in Tables 8 to 13.

In the VECTIS co-ordinates system, the new instrument positions are;

SONIC#1a	x = 73.57 m	y = 0.25 m	z = 3.80 m
SONIC#2a	x = 73.57 m	y = 0.25 m	z = 5.40 m
SONIC#3a	x = 73.57 m	y = 0.25 m	z = 8.00 m
SONIC#4a	x = 73.57 m	y = 0.25 m	z = 13.00 m
SONIC#5a	x = 73.57 m	y = 0.25 m	z = 20.00 m

4.b The vertical displacement and velocity error

At the SONIC#1a site the airflow has been raised by 0.12 m from its original height by the time it reaches the anemometer position (Table 8). The airflow has been raised by 0.13 m at the SONIC#2a site, 0.15 m at the SONIC#3a site, 0.31 m at the SONIC#4a site and 0.55 m at the SONIC#5a site (Tables 9 to 12 respectively).

Figures 13 to 17 show lines of data through the five anemometer positions and the kinks in the vertical profiles of velocity (Section 3.d) can be clearly seen. Again, the error in the estimate of the wind speed increases nearer the surface, with the maximum error less than 0.05 ms^{-1}. The velocity error

estimates at these sites are summarised in Table 13 along with the uncertainties in the error estimates. All the instrument sites experience small rates of change of velocity (Table 14).

Location	x (m)	y (m)	z (m)
P (SONIC#1a)	73.57	0.25	3.80
P_{stream}	73.57	0.25	3.79
$P-P_{stream}$	0.00	0.00	0.01
P_{origin}	392.89	0.25	3.66
$P_{stream}-P_{origin}$			$\Delta z=0.13$

Table 8 The vertical displacement, Δz, of the flow to the SONIC#1a anemometer.

Location	x (m)	y (m)	z (m)
P (SONIC#2a)	73.57	0.25	5.40
P_{stream}	73.57	0.25	5.39
$P-P_{stream}$	0.00	0.00	0.01
P_{origin}	392.96	0.25	5.26
$P_{stream}-P_{origin}$			$\Delta z=0.13$

Table 9 The vertical displacement, Δz, of the flow to the SONIC#2a anemometer.

Location	x (m)	y (m)	z (m)
P (SONIC#3a)	73.57	0.25	8.00
P_{stream}	73.57	0.25	7.00
$P-P_{stream}$	0.00	0.00	0.00
P_{origin}	392.64	0.25	7.85
$P_{stream}-P_{origin}$			$\Delta z=0.15$

Table 10 The vertical displacement, Δz, of the flow to the SONIC#3a anemometer.

Location	x (m)	y (m)	z (m)
P (SONIC#4a)	73.57	0.25	13.00
P_{stream}	73.57	0.25	12.99
$P-P_{stream}$	0.00	0.00	0.01
P_{origin}	392.76	0.25	12.68
$P_{stream}-P_{origin}$			$\Delta z=0.31$

Table 11 The vertical displacement, Δz, of the flow to the SONIC#4a anemometer.

Location	x (m)	y (m)	z (m)
P (SONIC#5a)	73.57	0.25	20.00
P_{stream}	73.57	0.25	20.00
$P-P_{stream}$	0.00	0.00	0.00
P_{origin}	392.74	0.25	19.45
$P_{stream}-P_{origin}$			$\Delta z=0.55$

Table 12 The vertical displacement, Δz, of the flow to the SONIC#5a anemometer.

Instrument site	Velocity from each direction	Average velocity (ms^{-1})	Free stream velocity (ms^{-1})	% Error
SONIC#1a	12.089(x) 12.093(y) 12.122(z)	12.101	13.805	-12.34 ± 0.26
SONIC#2a	12.562(x) 12.565(y) 12.587(z)	12.571	14.198	-11.46 ± 0.31
SONIC#3a	13.141(x) 13.144(y) 13.164(z)	13.150	14.712	-10.62 ± 0.29
SONIC#4a	14.014(x) 14.017(y) 14.033(z)	14.021	15.336	-8.57 ± 0.28
SONIC#5a	15.053(x) 15.054(y) 15.067(z)	15.058	15.959	-5.65 ± 0.04

Table 13 Wind speed errors at the instrument sites 14.2 m forward of the bow

Instrument site	Velocity data line	Rate of change of velocity per metre (ms^{-1}/m)	Rate of change of velocity per cell (ms^{-1}/cell)
SONIC#1a	Along (x)	0.098	0.033
	Across (y)	0.003	0.001
	Up (z)	0.342	0.058
SONIC#2a	Along (x)	0.087	0.029
	Across (y)	0.002	0.001
	Up (z)	0.284	0.048
SONIC#3a	Along (x)	0.082	0.029
	Across (y)	0.002	0.001
	Up (z)	0.263	0.042
SONIC#4a	Along (x)	0.074	0.028
	Across (y)	0.004	0.001
	Up (z)	0.211	0.034
SONIC#5a	Along (x)	0.026	0.011
	Across (y)	0.001	0
	Up (z)	0.157	0.026

Table 14 Rate of change of velocity close to the anemometer sites 14.2 m forward of the bow.

5. Summary

The distortion of the air flow to the instrument sites on the *F.S. Polarstern* has been quantified for a 10 m wind speed of 15 ms^{-1} blowing directly over the bow of the ship. It should be noted that the effects of the flow distortion can vary rapidly with a change in the relative wind direction (Yelland *et al.,* 1998), i.e. these results are valid for a bow on flow only. The distortion of the flow is only that due to the ship's superstructure and hull, since small scale structures (the lattice tower) and very local obstructions (the other instruments) can not be modelled.

The vertical displacement (Δz) of the flow was used to get an effective anemometer height ($z-\Delta z$), and the wind speed error relates the actual flow at the instrument site to the free steam velocity at this effective height. This approach is required if the wind speed data from an anemometer are used to calculate

the wind stress via the dissipation method (Yelland *et al.,* 1998). The results for all the instruments are summarised in Table 15. If the actual (rather than the effective) height of the instrument is used to obtain the free stream velocity then the wind speed error at the instrument site will change accordingly. Table 16 shows the results for each instrument if the free stream velocity is calculated in this way.

The vertical displacement of the flow is due to the large structure of the ship's hull and is sensitive to the instrument location. The vertical displacement increases with height and decreases with distance in front of the ship. When the anemometers are positioned 11.2 m in front of the bow, the vertical displacement ranges from 0.16 m at the SONIC#1 site (3.8 m height) to 0.68 m at the SONIC#5 site (20 m height). When the anemometers are moved further upwind, to a position 14.2 m in front of the bow, the vertical displacements become slightly smaller (e.g. a displacement of 0.55 m is found at the SONIC#5a site).

The effect of flow distortion on the velocity is also sensitive to position, with the wind speed error decreasing both with height and with distance in front of the bows. At the SONIC#1 position (11.2 m upwind of the bow) the flow has been decelerated by about 15 %, and the deceleration reduces to about 12 % at the SONIC#1a site 14.2 m upwind of the bow. The SONIC#5a site at a height of 20 m and a distance of 14.2 m upwind experience the least deceleration, about 6 %.

Instrument	Instrument height z (m)	Velocity at instrument site (ms^{-1})	Free stream velocity (at $z - \Delta z$) (ms^{-1})	% velocity error at instrument site	Vertical displacement Δz (m)	Angle of flow to the horizontal (degrees)
11.2 m forward of the bow						
SONIC#1	3.8	11.716	13.809	**-15.16 ± 0.20 (0.23)**	**0.16**	**1.2**
SONIC#2	5.4	11.236	14.204	**-13.85 ± 0.26 (0.18)**	**0.18**	**1.5**
SONIC#3	8.0	12.836	14.711	**-12.74 ± 0.30 (0.16)**	**0.23**	**2.0**
SONIC#4	13	13.734	15.344	**-10.49 ± 0.15 (0.05)**	**0.41**	**2.1**
SONIC#5	20	14.985	15.946	**-6.03 ± 0.11 (0.08)**	**0.68**	**2.9**
14.2 m forward of the bow						
SONIC#1a	3.8	12.101	13.805	**-12.34 ± 0.26 (0.42)**	**0.12**	**0.9**
SONIC#2a	5.4	12.571	14.198	**-11.46 ± 0.31 (0.34)**	**0.13**	**1.2**
SONIC#3a	8.0	13.150	14.712	**-10.62 ± 0.29 (0.29)**	**0.15**	**1.5**
SONIC#4a	13	14.021	15.336	**-8.56 ± 0.28 (0.22)**	**0.31**	**2.0**
SONIC#5a	20	15.058	15.959	**-5.65 ± 0.04 (0.16)**	**0.55**	**2.3**

Table 15 Summary of the results for all instrument sites on the *F.S. Polarstern*. The figures in brackets indicate the maximum rate of change of velocity per cell (expressed as a percentage of the free stream velocity) for each site.

Instrument	Instrument height, z (m)	Velocity at instrument (ms^{-1})	Free stream velocity at height z (ms^{-1})	% velocity error at instrument site
11.2 m forward of the bow				
SONIC#1	3.8	11.716	13.857	-15.45
SONIC#2	5.4	12.236	14.252	-14.14
SONIC#3	8.0	12.836	14.748	-12.96
SONIC#4	13.0	13.734	15.385	-10.73
SONIC#5	20.0	14.985	15.999	-6.34
14.2 m forward of the bow				
SONIC#1a	3.8	12.101	13.842	-12.58
SONIC#2a	5.4	12.571	14.232	-11.67
SONIC#3a	8.0	13.150	14.731	-10.73
SONIC#4a	13.0	14.021	15.367	-8.76
SONIC#5a	20.0	15.058	15.996	-5.86

Table 16 The wind speed errors calculated using a free stream velocity at the actual instrument height, z.

The two sources of errors in the results presented here are due to the mesh resolution and the extraction of the data. The mesh resolution errors are due to the region of fine mesh not being extended far enough upstream and have been quantified by fitting curves to the data and calculating the errors. All the uncertainties due to the mesh resolution are very small, with the largest equating to ±0.3 % of the wind speed at the SONIC#1a site.

Table 7 showed that the maximum variation in velocity from one cell to the next in the location of the instruments (at 11.2 m upwind of the bow) varies from about 0.01 ms^{-1}/cell at the SONIC#5 site up to 0.032ms^{-1}/cell at the SONIC#1 site. These values, plus those for the anemometer positions at 14.2 m forward of the bow, are expressed as a percentage of the free stream flow and are shown in brackets in Table 15. Combining these two sources of error gives a maximum uncertainty in the wind speeds of ±0.7 % and an average uncertainty of ±0.4 %.

Overall, all the anemometer sites experience moderate to severe flow distortion, with the wind speeds decelerated by up to 15% and displaced vertically by up to 0.6m. The best results are found with

increasing distance from the bows and with increasing height. However, even the best exposed site at SONIC#5a, 14.2 m upwind and 20 m high, experiences decelerations of 6%. It is estimated that for an anemometer at a height of 8 m (the height of SONIC#3), the deceleration of the flow would decrease to 5 % at a distance of about 30 m upwind of the bow, and to 1 % about 80 m or more upwind.

6. References

Moat, B. I., M. J. Yelland, and J. Hutchings, 1996: Airflow over the *R.R.S. Discovery* using the Computational Fluid Dynamics package VECTIS, SOC Internal Report No. 2, Southampton Oceanography Centre, Southampton, UK. 41 pp.

Yelland, M. J., B. I. Moat, P. K. Taylor, R. W. Pascal, J. Hutchings, and V. C. Cornell, 1998: Wind stress measurements from the open ocean corrected for air-flow distortion by the ship, *Journal of Physical Oceanography* **28**, 1511 - 1526.

7. Figures

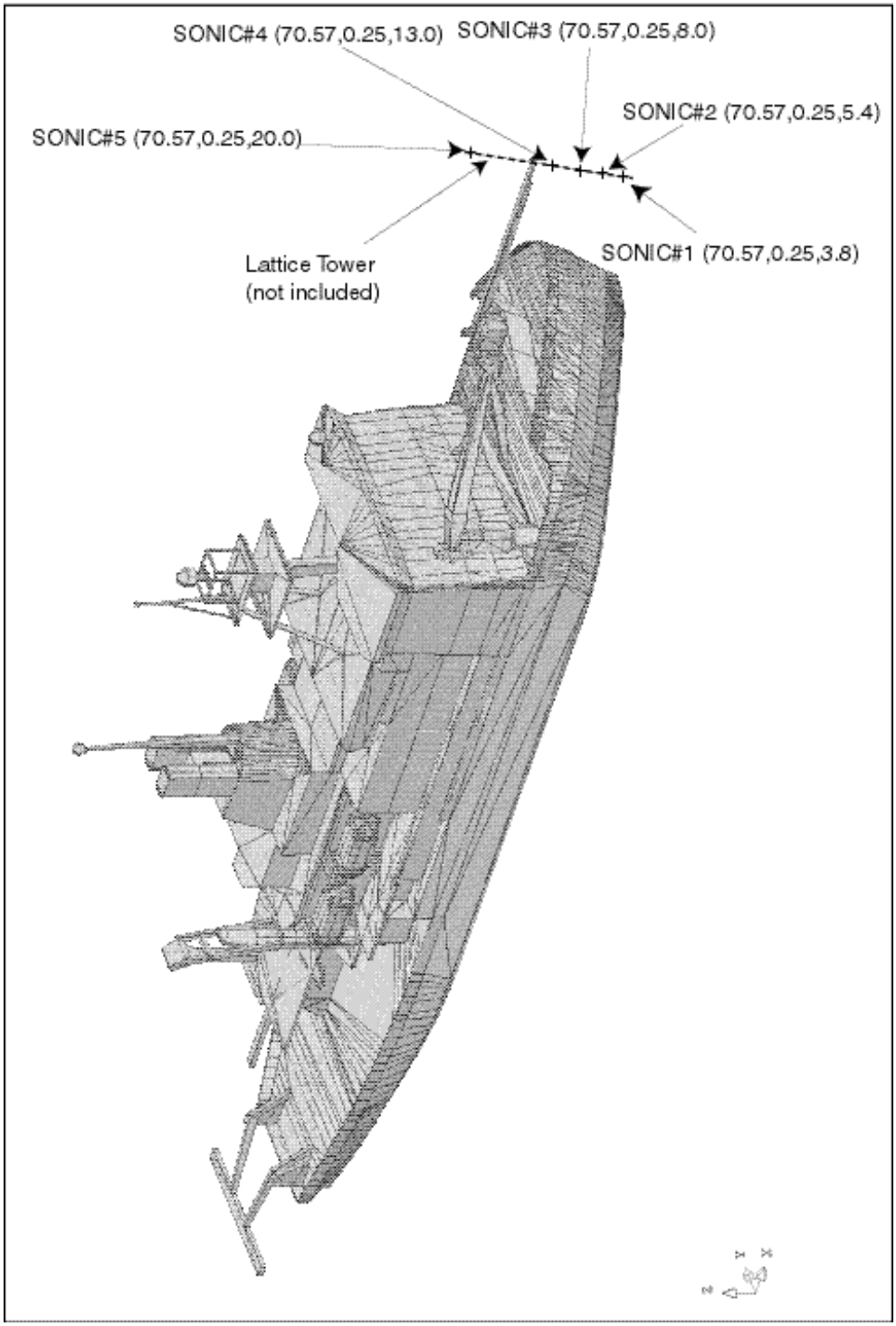

Figure 1. A 3-dimensional view of the *F.S. Polarstern.* The x, y, z coordinates of the anemometers are shown.

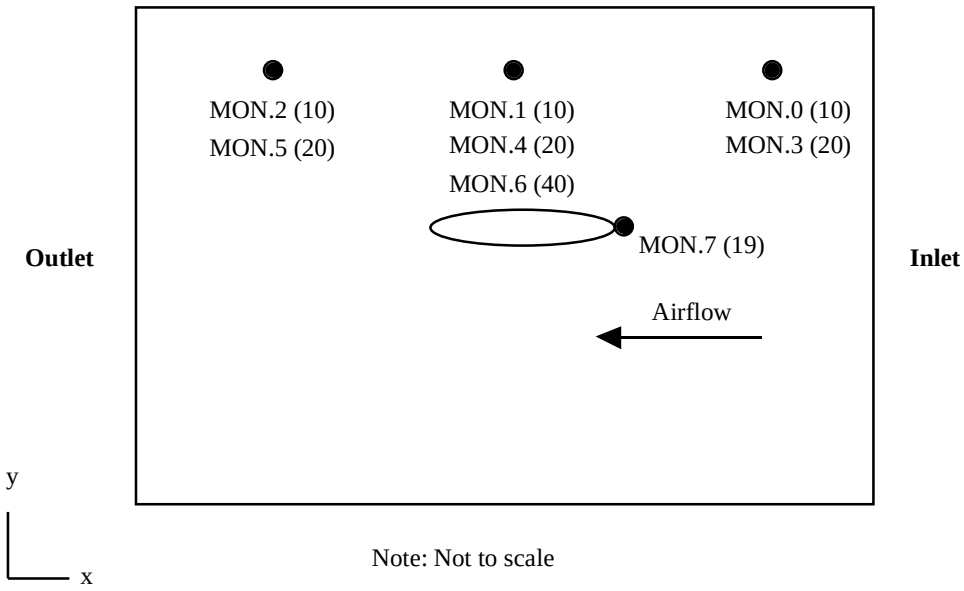

Figure 2. Schematic plan view of the wind tunnel used to simulate a flow of air over the bows of the *F.S. Polarstern*. The monitoring points are shown by the solid circles and their heights in metres are indicated in brackets.

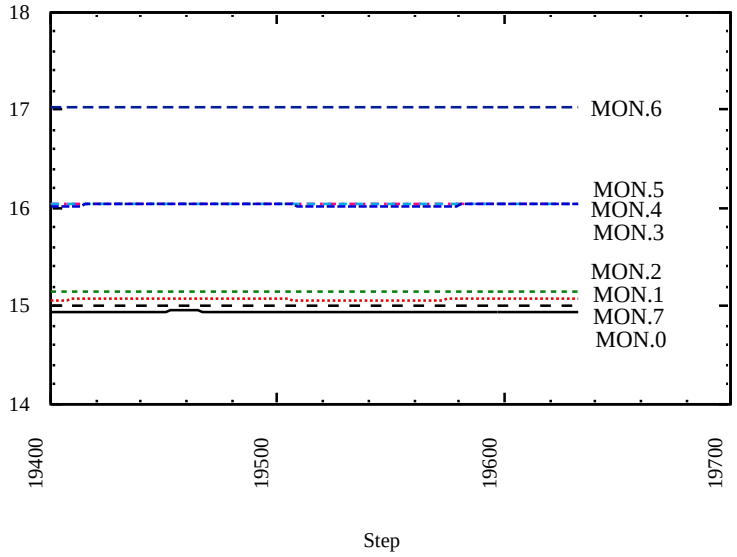

Figure 3. Velocity data from the eight monitoring locations for the last 250 time steps

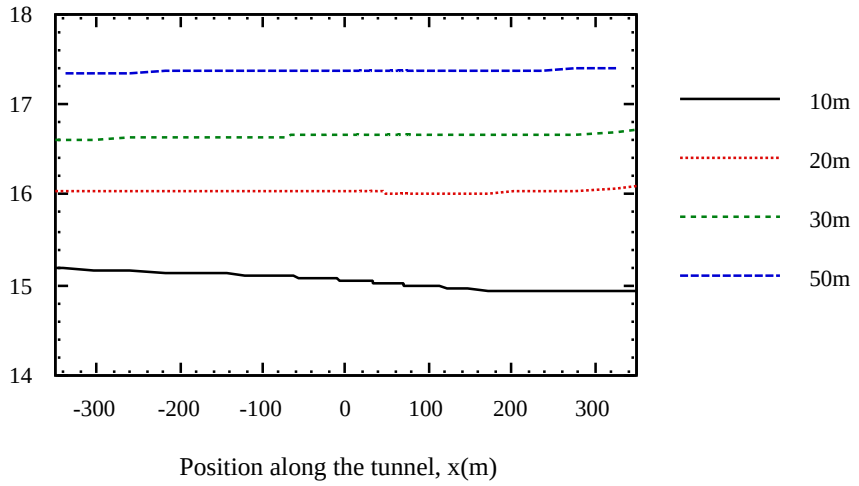

Figure 4a. Lines of velocity data along the length of the tunnel at the heights shown. The data were obtained from the free stream region on the port side of the tunnel at y = 250m.

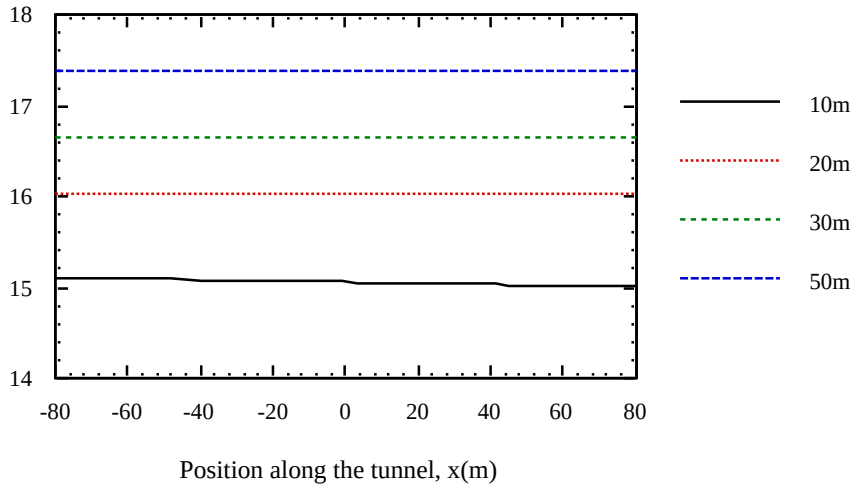

Figure 4b. As Fig. 4a, showing the central portion of the tunnel only.

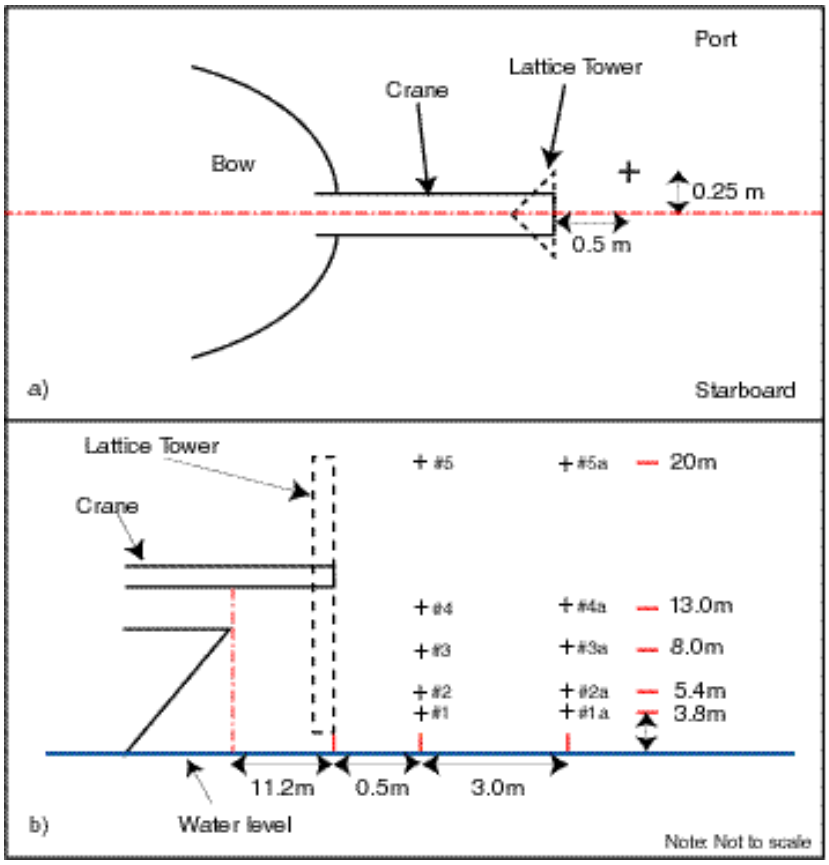

Figure 5. Schematic of the SONIC instrument positions relative to the lattice tower and bows of the *F.S. Polarstern*; a) plan view and b) side view. N.B. the lattice tower itself is not modelled.

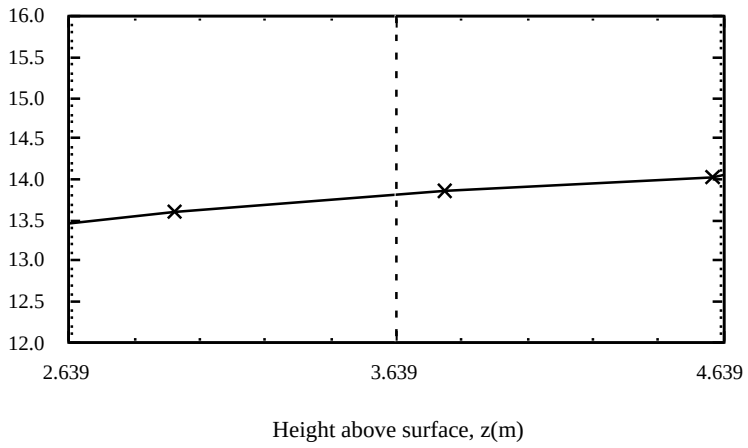

Figure 6. The vertical profile of velocity abeam of the SONIC#1 anemometer site. The dashed line indicates the height at which the air flow originated.

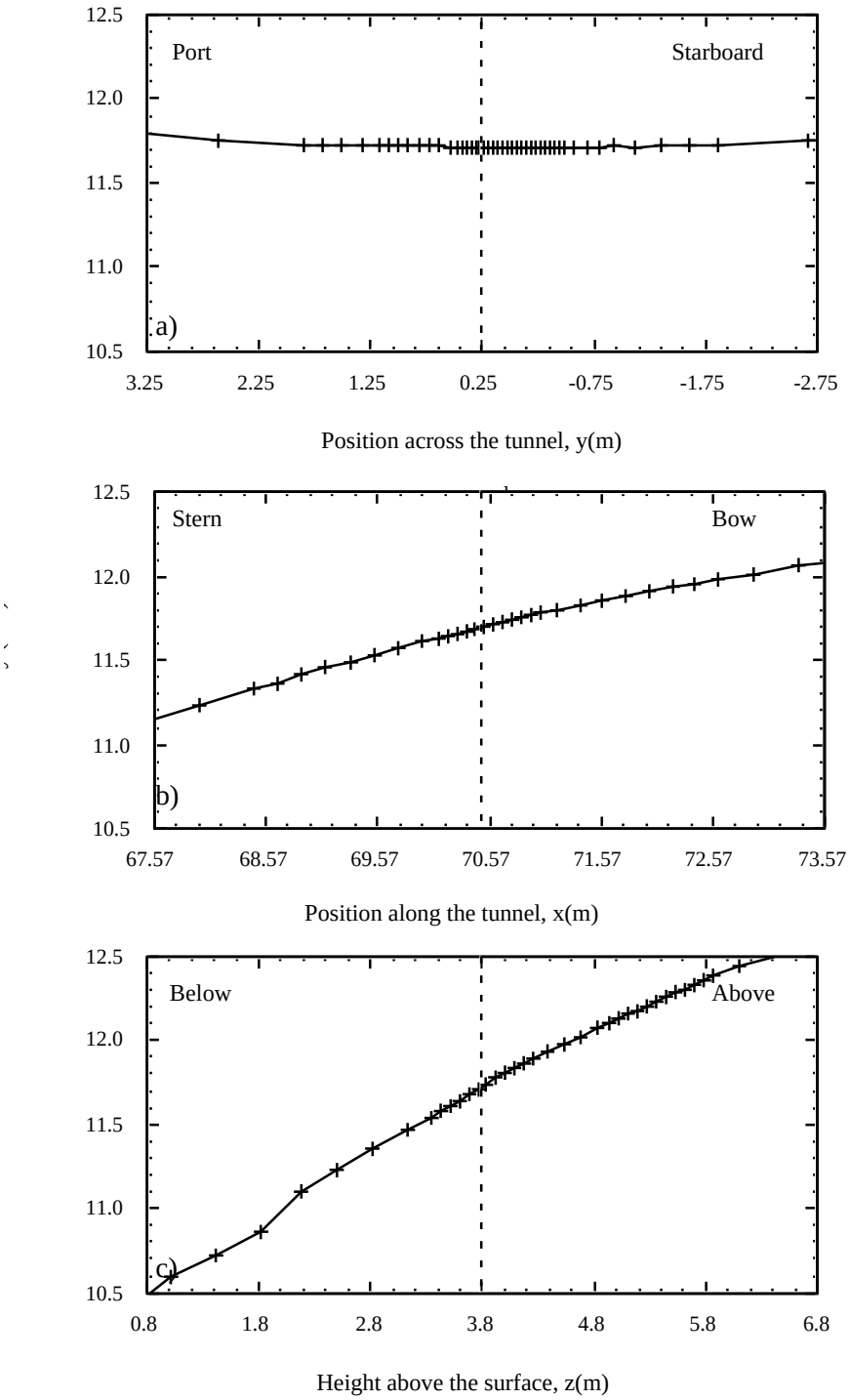

Figure 7. Lines of velocity data through the SONIC#1 position (indicated by the dashed line) in all three directions; a) across the tunnel (y); b) along the tunnel (x) and c) vertically(z).

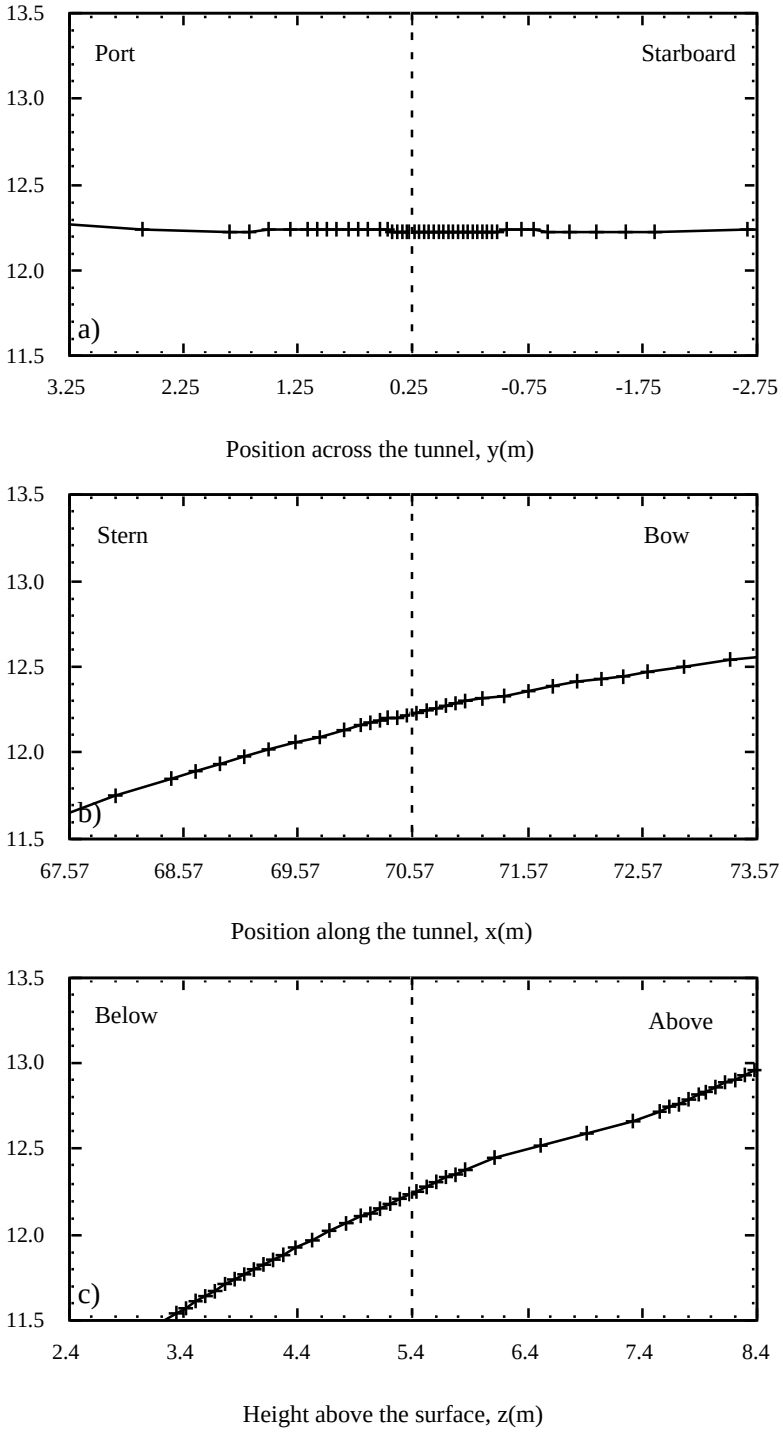

Figure 8. As for Figure 7, but for the SONIC#2 anemometer site.

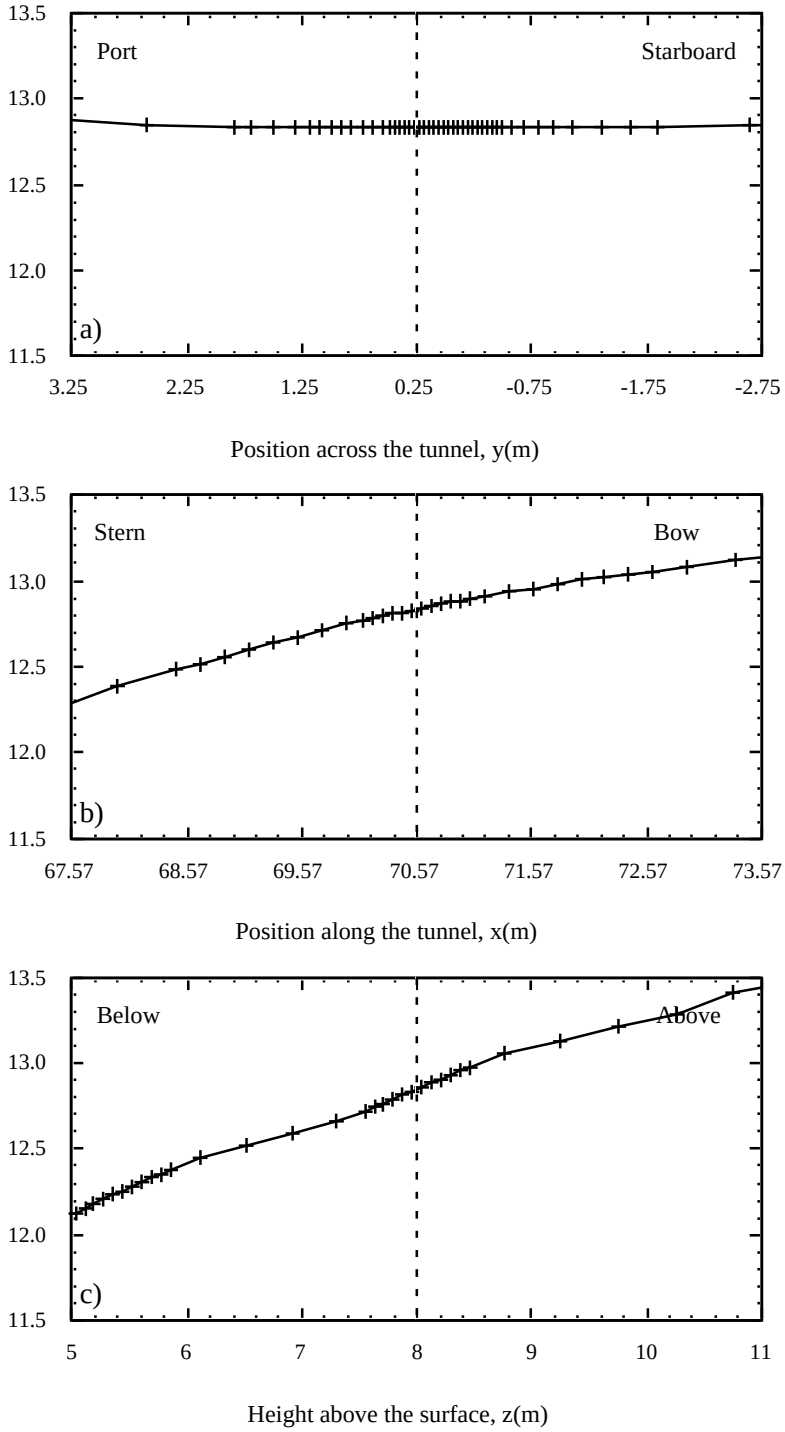

Figure 9. As for Figure 7, but for the SONIC#3 anemometer site.

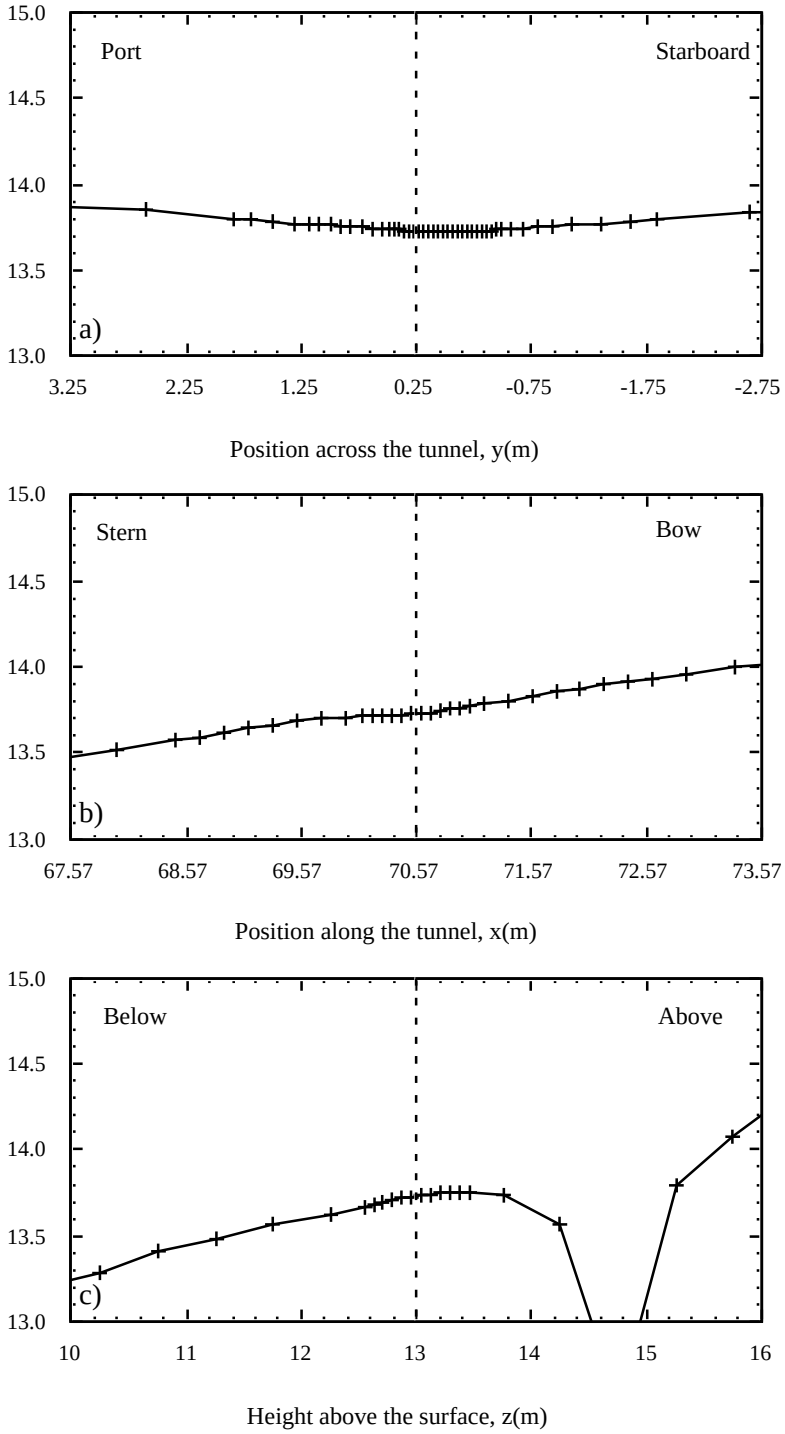

Figure 10. As for Figure 7, but for the SONIC#4 anemometer site.

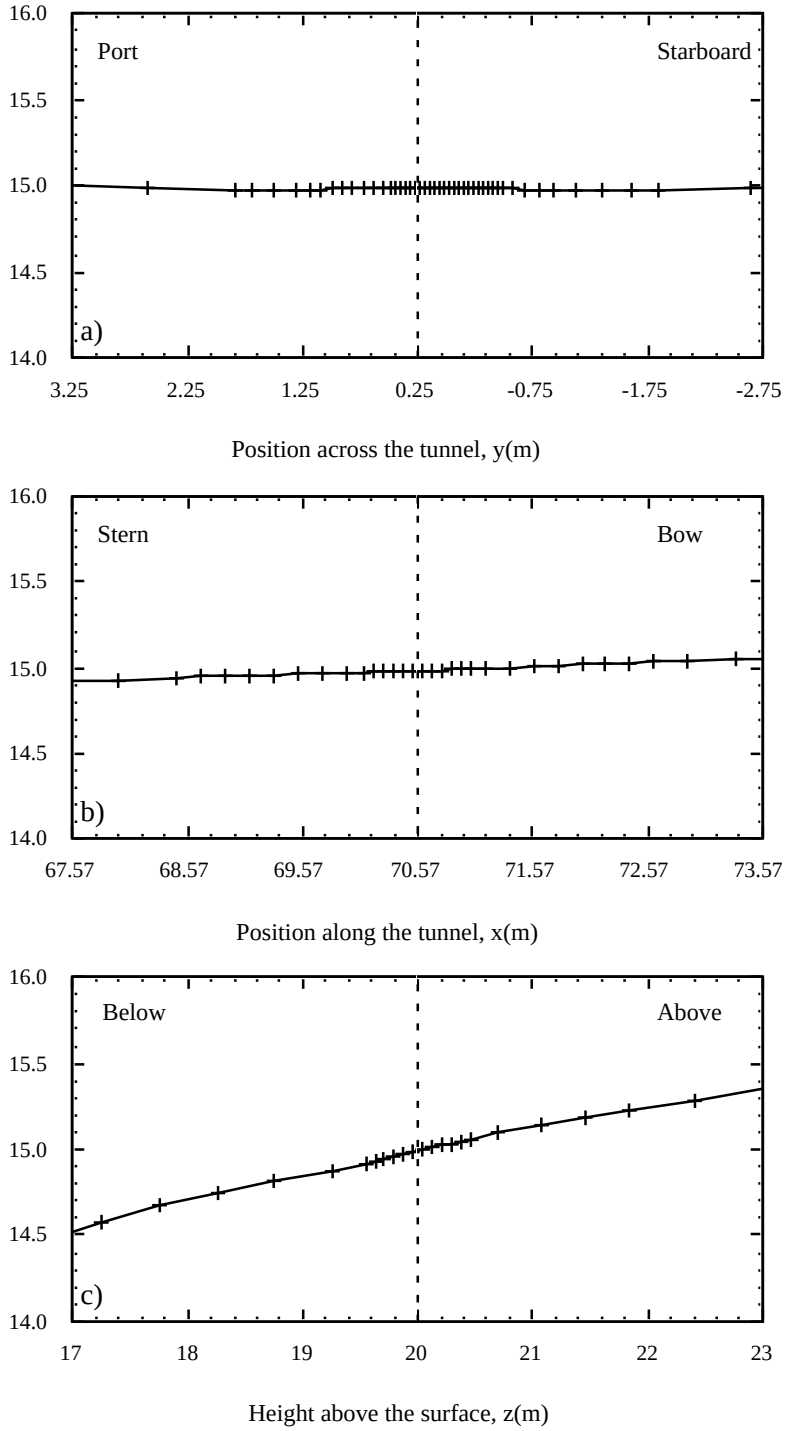

Figure 11. As for Figure 7, but for the SONIC#5 anemometer site.

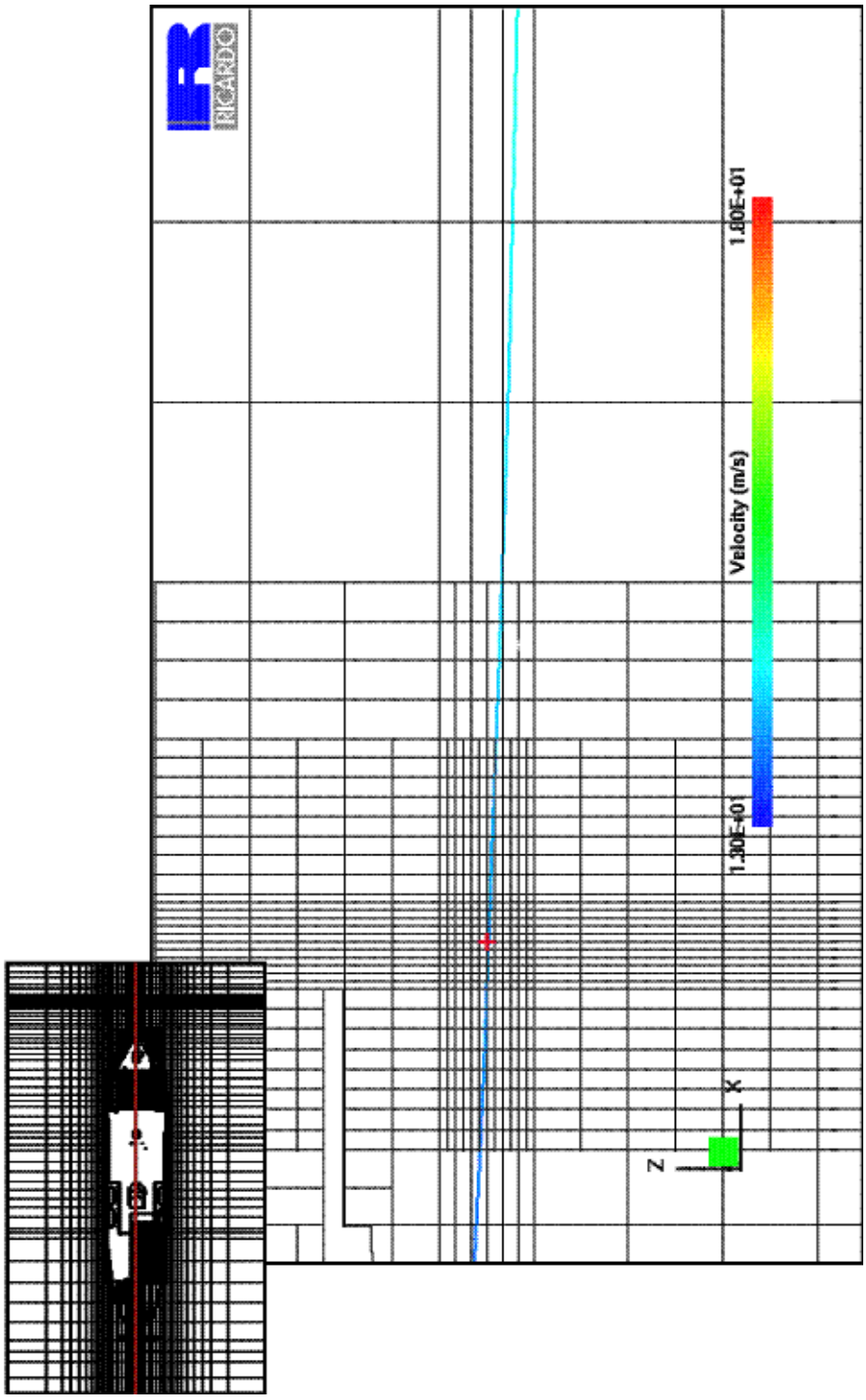

Figure 12. Close up of the SONIC#3 anemometer position (red +) showing the rapid increase in cell size upstream of the instrument sites.

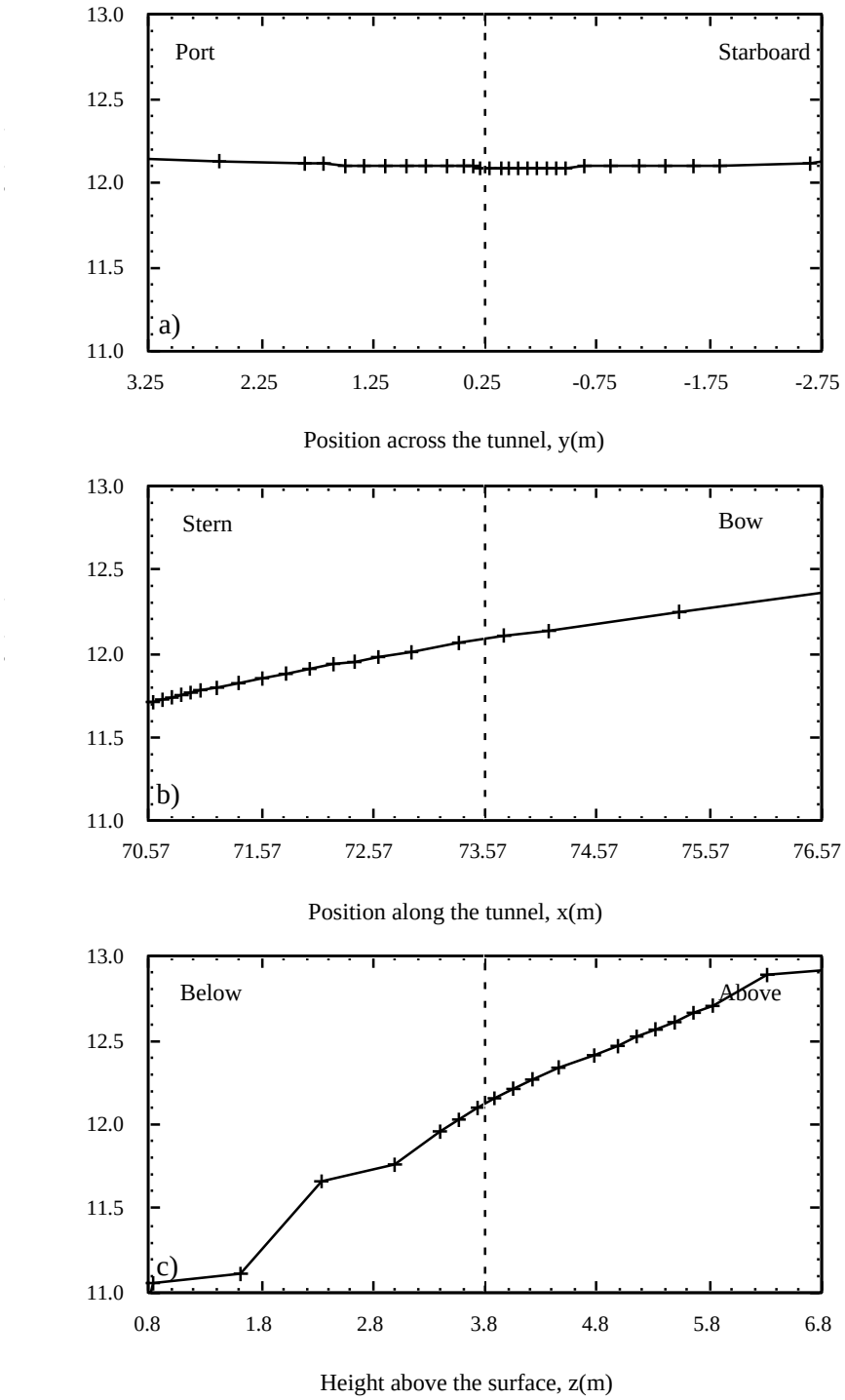

Figure 13. As for Figure 7, but for the SONIC#1a anemometer site 14.2 m forward of the bow

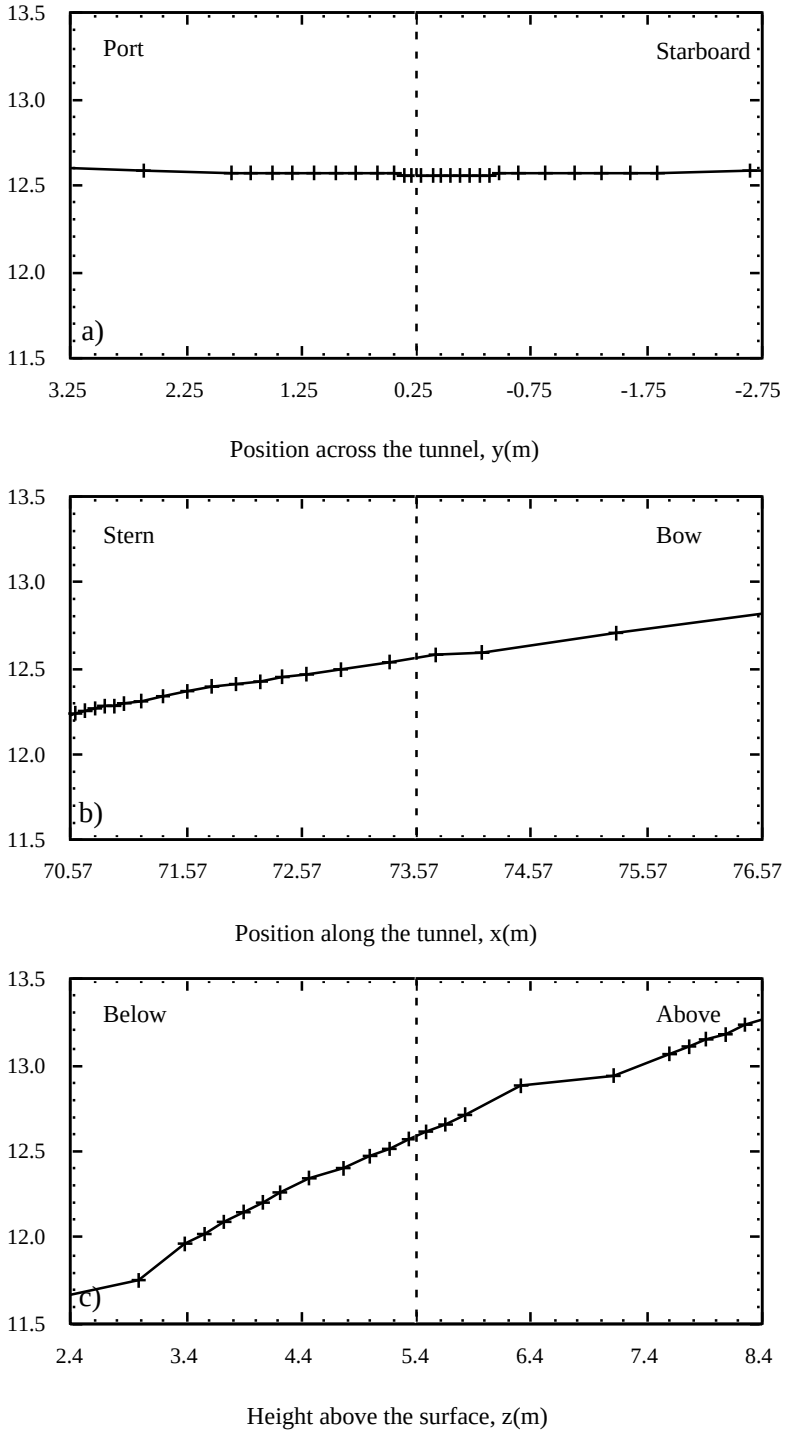

Figure 14. As for Figure 13, but for the SONIC#2a anemometer site.

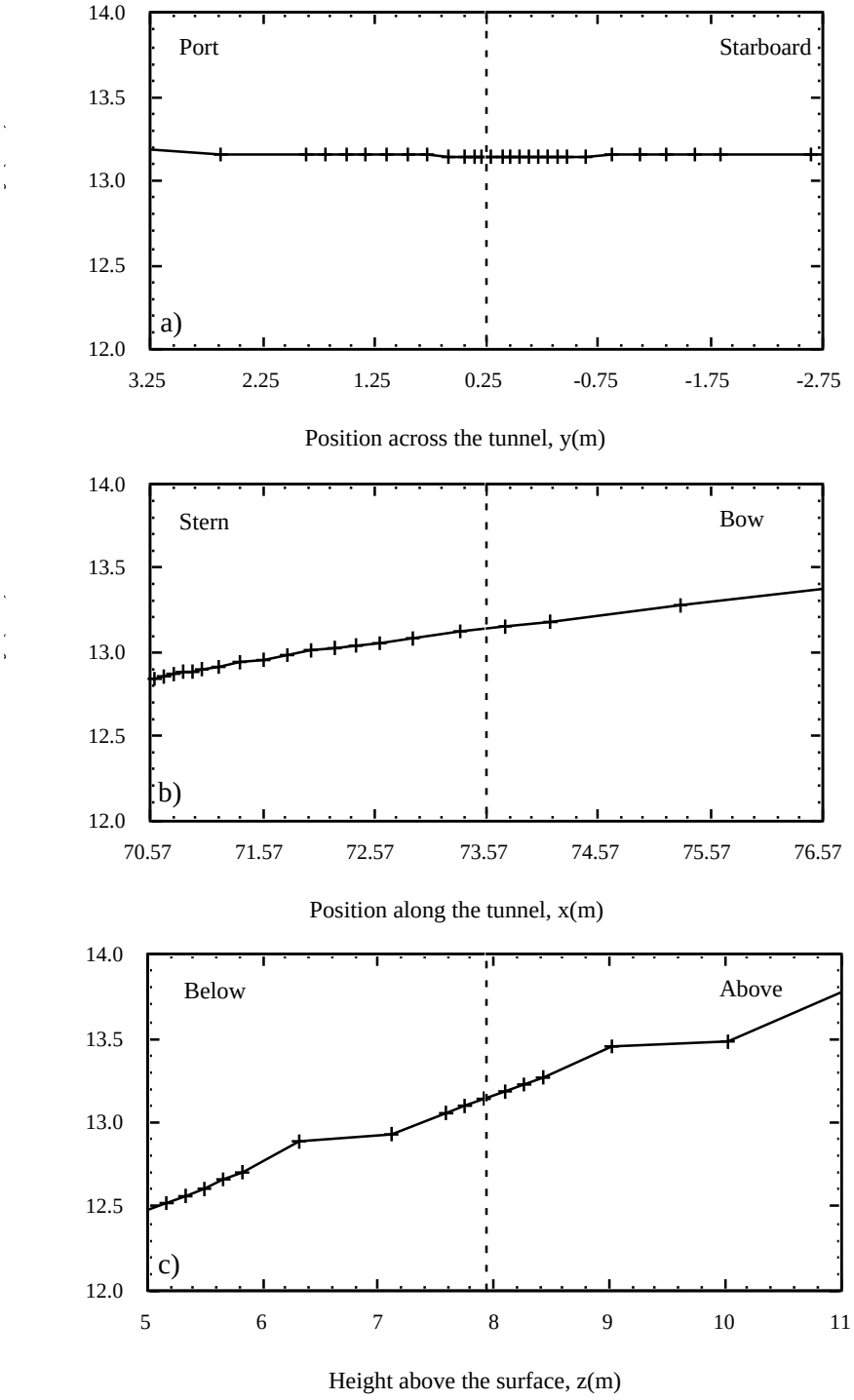

Figure 15. As for Figure 13, but for the SONIC#3a anemometer site.

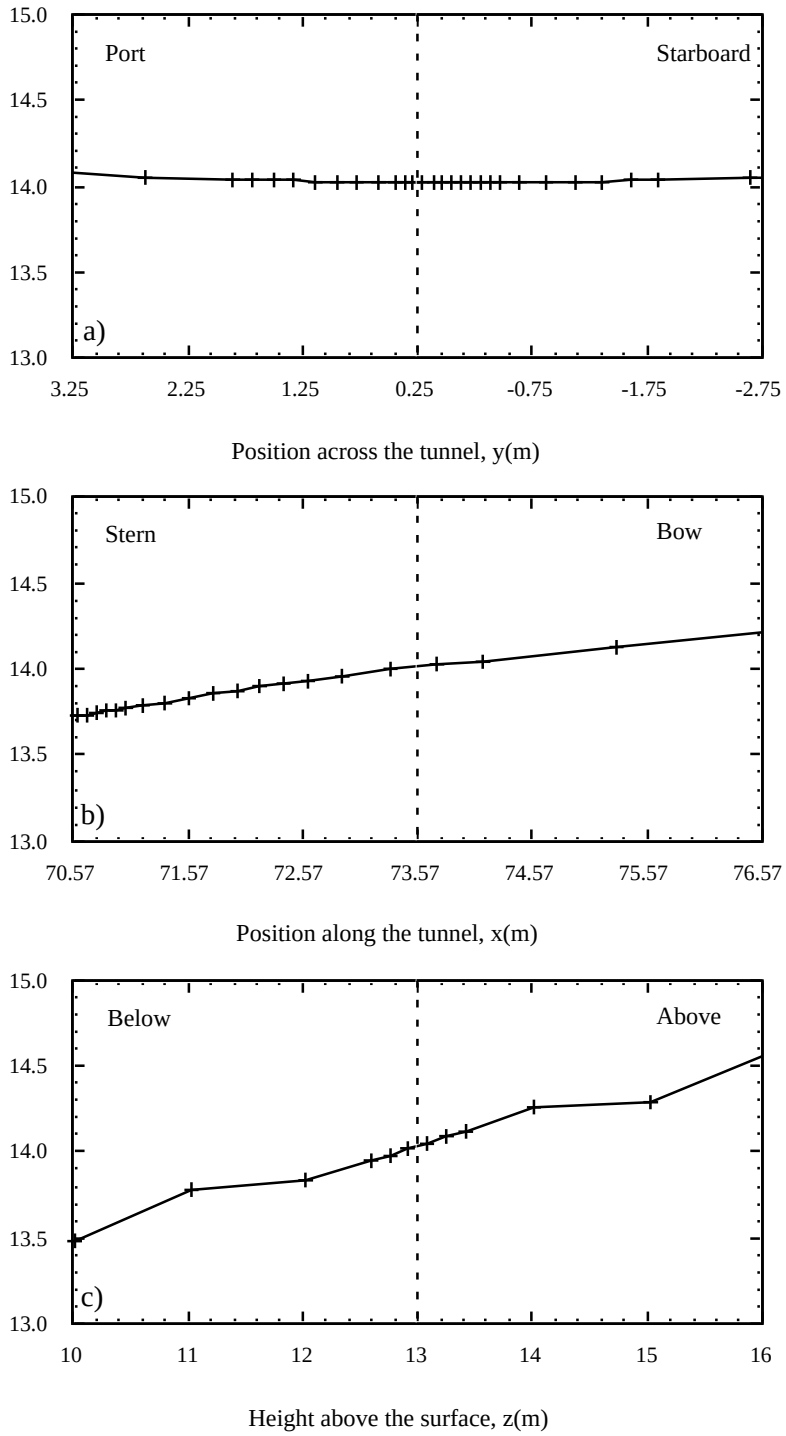

Figure 16. As for Figure 13, but for the SONIC#4a anemometer site.

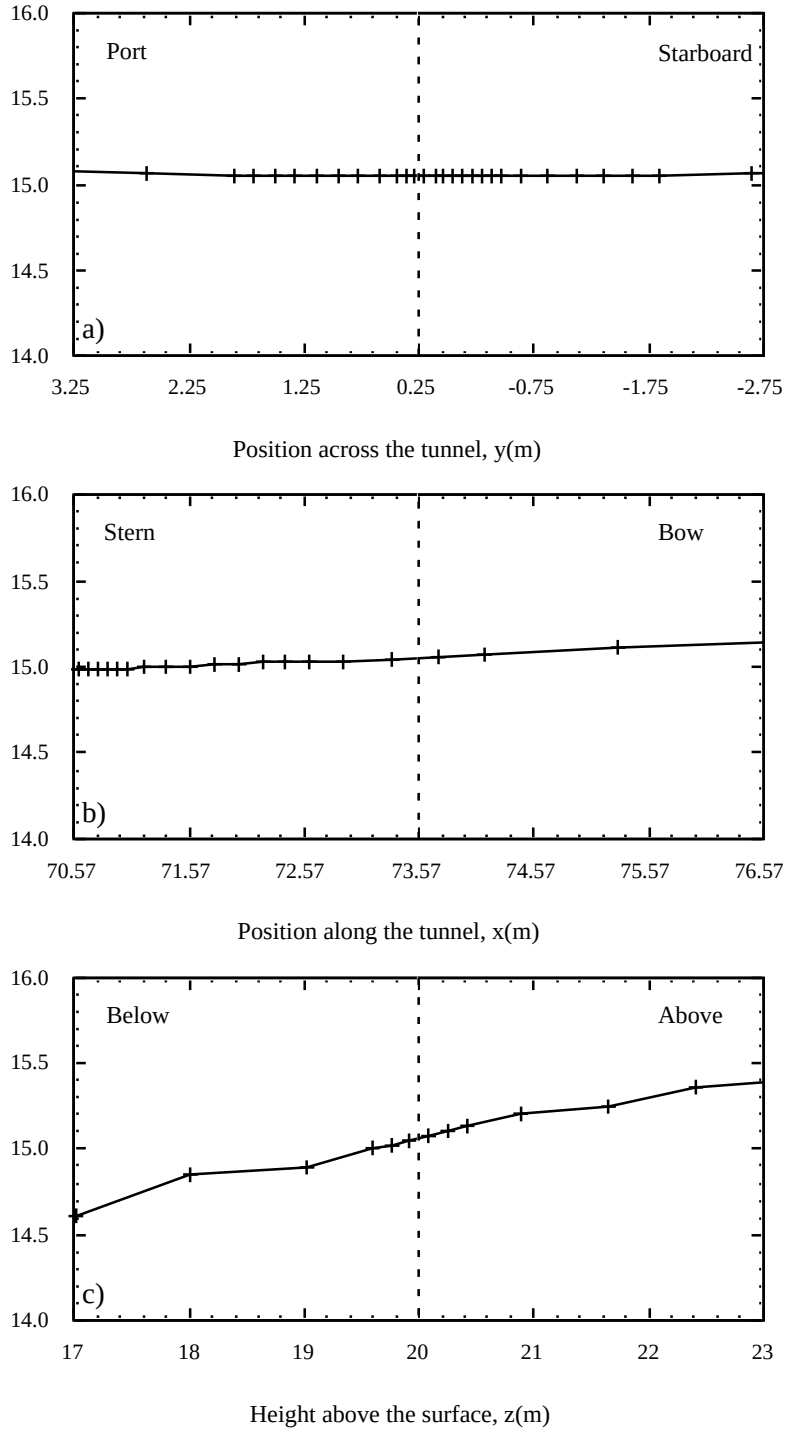

Figure 17. As for Figure 13, but for the SONIC#5a anemometer site.

8. Appendix

The Figures in this Appendix were generated using the VECTIS post-processing software. Each Figure shows data on a major plane, and the orientation of the plane is indicated by a red line in the small box at the top left of each Figure. The variable size of the computational cells can be seen in all the Figures.

FIGURE A1 Velocity vectors on a vertical plane through the instrument sites. The magnitude of the total velocity is indicated by the colour of the arrows. The length and direction of the arrows represent the magnitude and direction of the component of the velocity in the plane of view. Each arrow represents the result from one computational cell. The positions of the instruments are indicated by crosses and the velocity scale corresponds to 13 ms^{-1} to 18 ms^{-1}.

FIGURE A2 As Figure A1 for a vertical section across the tunnel which intersects the instrument sites 11.2 m forward of the bow(indicated by the crosses).

FIGURE A3 As Figure A1 for a vertical section across the tunnel which intersects the instrument sites 14.2 m forward of the bow(indicated by the crosses).

FIGURE A4 As Figure A1 for a horizontal section through the SONIC#4 and SONIC#4a instrument sites (indicated by the crosses).

FIGURE A5 A streamline, or massless particle trace, which passes through the SONIC#4 (13 m H eight) anemometer site (indicated by the white '+'). The blue '+' signs indicate the position of the other anemometers 11.2 m forward of the bow at 3.8 m (SONIC#1), 5.4 m (SONIC#2), 8.0 m (SONIC#3) and 20 m height (SONIC#5). The red crosses mark the SONIC#1a to SONIC#5a sites.

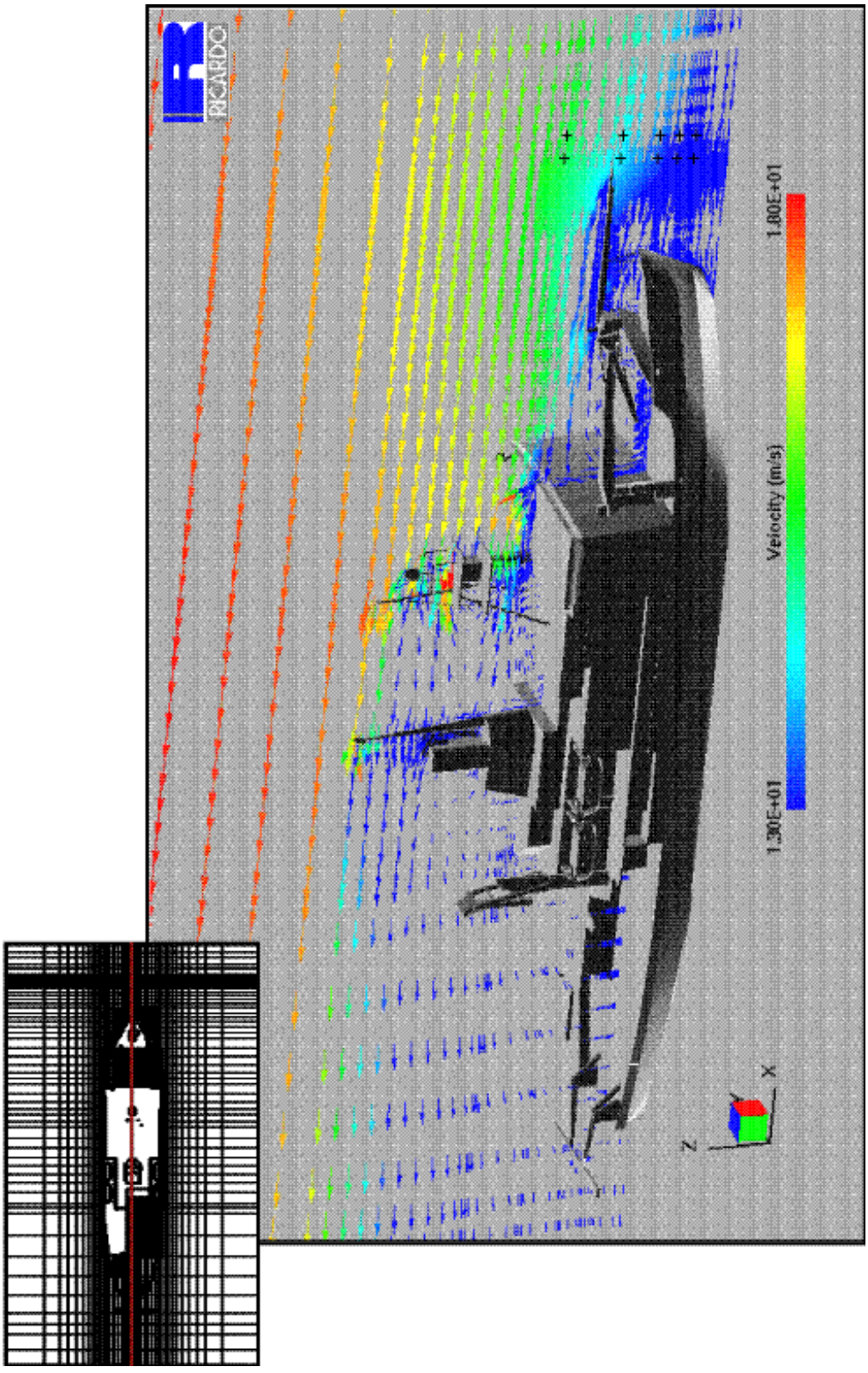

Figure A1

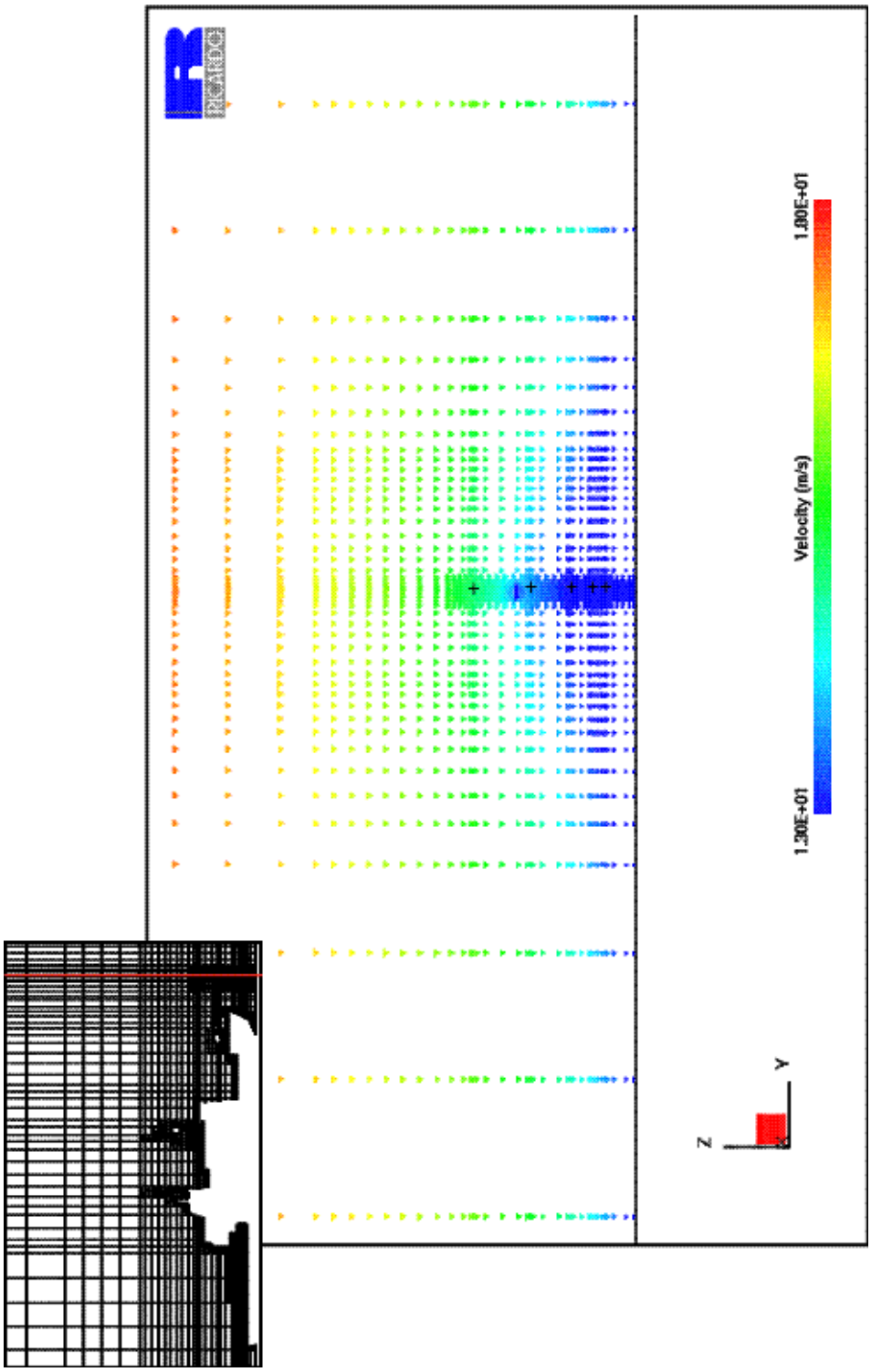

Figure A2

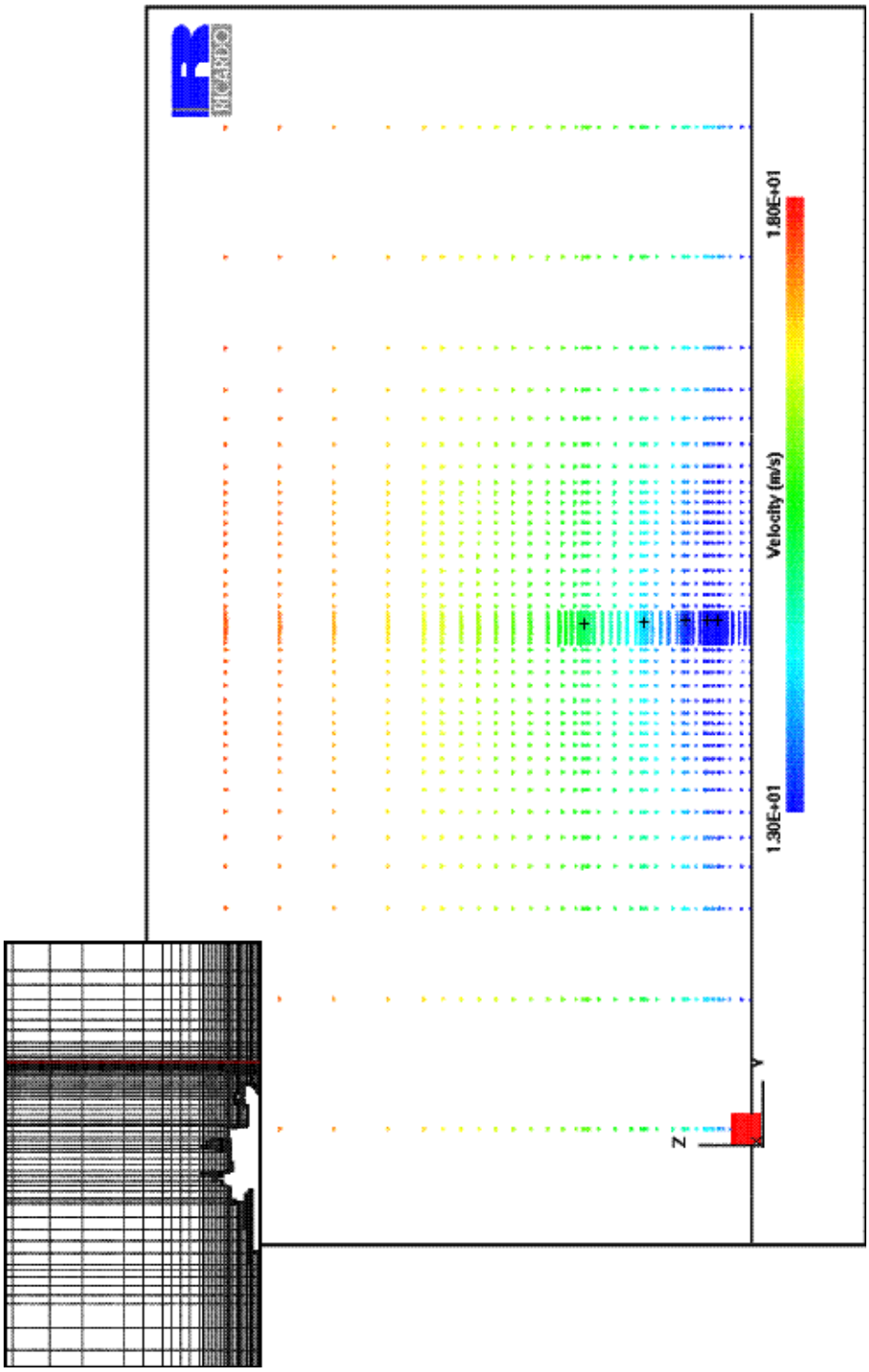

Figure A3

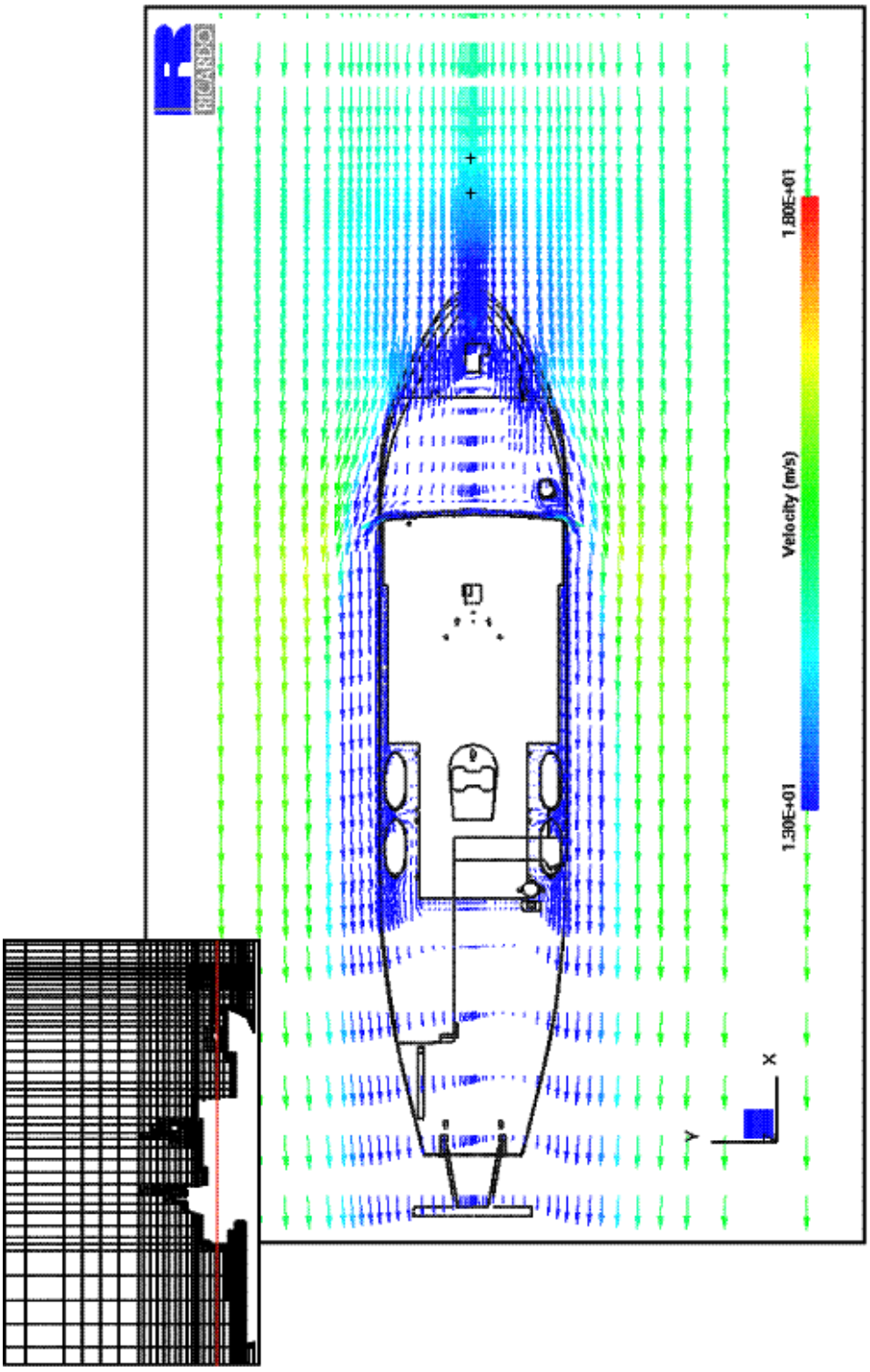

Figure A4

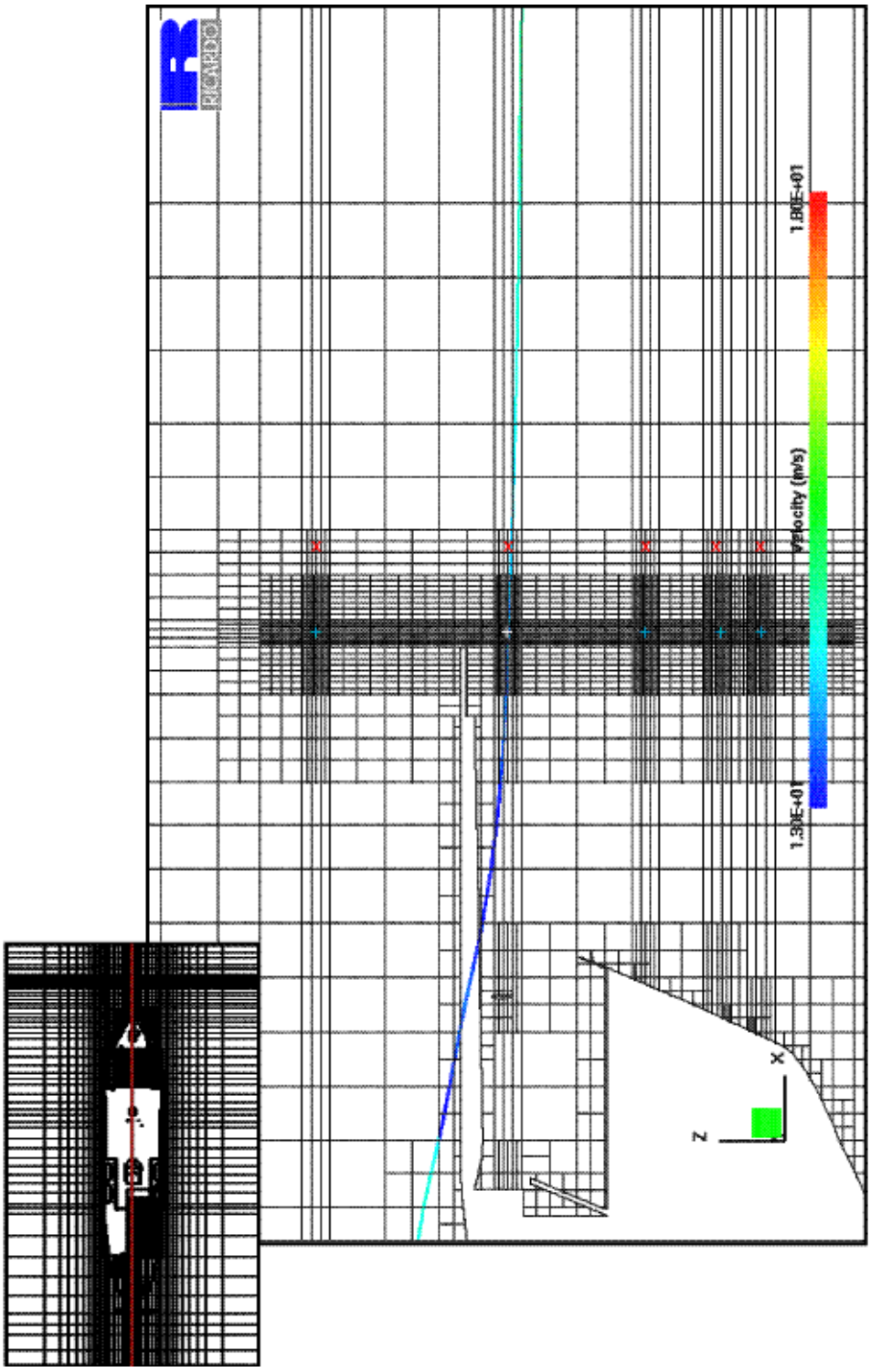

Figure A5